Observations of kinetic ballooning/interchange instability signatures in the magnetotail

E. V. Panov,[1] V. A. Sergeev,[2] P. L. Pritchett,[3] F. V. Coroniti,[3] R. Nakamura,[1] W. Baumjohann,[1] V. Angelopoulos,[4] H. U. Auster,[5] and J. P. McFadden[6]

Received 12 March 2012; revised 29 March 2012; accepted 29 March 2012; published 26 April 2012.

[1] Stimulated by a recent study of a kinetic ballooning/interchange instability by Pritchett and Coroniti (2010), we present THEMIS events that confirm the predictions of this mechanism. In these events the probes were situated in the plasma sheet at 11 Re, near the presumed location of a B minimum. Prior to substorm onset, they observed strong magnetic oscillations with periods 20–100 s and δB_X about 10–20 nT. Associated with these were oscillations of the electric field $\delta E_Y \sim 1$ mV/m and the field-aligned electron velocity of several hundreds of km/s. No comparable perturbations in the ion velocity were observed. For two cases cross-correlation analyses proved duskward propagation of the elongated spatial structures with a cross-tail width of a few ion gyroradii and a propagation velocity of about the ion drift velocity. In one case THEMIS probes confirmed a sausage-like geometry of the structures. **Citation:** Panov, E. V., V. A. Sergeev, P. L. Pritchett, F. V. Coroniti, R. Nakamura, W. Baumjohann, V. Angelopoulos, H. U. Auster, and J. P. McFadden (2012), Observations of kinetic ballooning/interchange instability signatures in the magnetotail, *Geophys. Res. Lett.*, *39*, L08110, doi:10.1029/2012GL051668.

1. Introduction

[2] Although reconnection is the major explosive energy dissipation mechanism during substorms [see, e.g., *Miyashita et al.*, 2009], substorm onset triggering and location are still debated. It has been argued, for example, that the onset may be initiated in thin current sheets around 15–30 R_E, or by a current disruption instability (CDI) between 6 and 10 R_E [see, e.g., *Ohtani*, 2004].

[3] Even though the region between 10 and 15 R_E has been sparsely explored, it may be of major importance for substorm onset triggering. *Saito et al.* [2010] presented evidence of local magnetic field minimum formation in the equatorial region near 11 Re at the end of a substorm growth phase. A configuration with such a minimum in the equatorial plane contains a tailward gradient of B_Z and may be unstable to a kinetic ballooning/interchange instability (BICI), amongst others [*Pritchett and Coroniti*, 2010, hereinafter PC2010]. Such an instability may generate azimuthally-localized, dipolarization-like intrusions of underpopulated plasma tubes into the inner magnetosphere and may provoke reconnection onset [*Pritchett and Coroniti*, 2011].

[4] Ballooning/interchange processes have long been substorm onset instability candidates [*Roux et al.*, 1991; *Cheng and Lui*, 1998]. As yet, however, there is no consensus about their physics, intensity, and significance for auroral breakup and reconnection onset. The clearest observational support comes from observations of azimuthally-spaced auroral forms (AAF) activated during breakup initiation. The mode numbers lie in a wide range, between 30 and 135 according to *Elphinstone et al.* [1995] and between 100 and 300 according to *Liang et al.* [2008]. Both westward and eastward propagations were reported, and azimuthal structuring was found both prior to breakup and during its initial stage [*Elphinstone et al.*, 1995; *Uritsky et al.*, 2009], giving the impression that different modes can contribute to this wide class of AAFs.

[5] So far it has been difficult to identify ballooning perturbations using *in situ* observations during the turbulent dipolarization that accompanies breakup because of the complexity and mix of different perturbations during that time. Recently, *Baumjohann et al.* [2007] and *Saito et al.* [2008] reported that plasma sheet oscillations observed before breakup and dipolarization may be produced by a ballooning/interchange instability.

[6] The THEMIS [*Angelopoulos*, 2008] probes clustered at around 10–12 R_E (P3, P4, P5) make it possible for us to directly investigate cross-tail size and propagation velocity. We also have collected more evidence of the kinetic nature of ballooning/interchange perturbations and discuss their consistency with BICI signatures. To emphasize the generality of our results, we illustrate three previously published events. We use observations from the three near-Earth probes (P3, P4, P5); during 2008 P3 and P4 moved along nearly the same orbit and near their apogee at ~12 R_E were separated by 0.8 R_E mostly in Y (or by ~0.2 h MLT). This separation is favorable for studying cross-tail structure and wave propagation. We use observations provided by the FGM [*Auster et al.*, 2008], ESA [*McFadden et al.*, 2008], and EFI [*Bonnell et al.*, 2008] instruments.

2. Signatures of Kinetic BICI From PC2010 Run

[7] Figure 1 shows field and plasma parameters from the PC2010 particle-in-cell run simulating a kinetic ballooning/

[1]Space Research Institute, Austrian Academy of Sciences, Graz, Austria.
[2]Earth Physics Department, St. Petersburg State University, St. Petersburg, Russia.
[3]Department of Physics and Astronomy, University of California, Los Angeles, California, USA.
[4]Institute of Geophysics and Planetary Physics, University of California, Los Angeles, California, USA.
[5]Institut für Geophysik und extraterrestrische Physik, Technische Universität Braunschweig, Braunschweig, Germany.
[6]Space Science Laboratory, University of California, Berkeley, California, USA.

Corresponding Author: E. V. Panov, Space Research Institute, Austrian Academy of Sciences, Schmiedlstraße 6, A-8042 Graz, Austria. (evgeny.panov@oeaw.ac.at)

0094-8276/12/2012GL051668

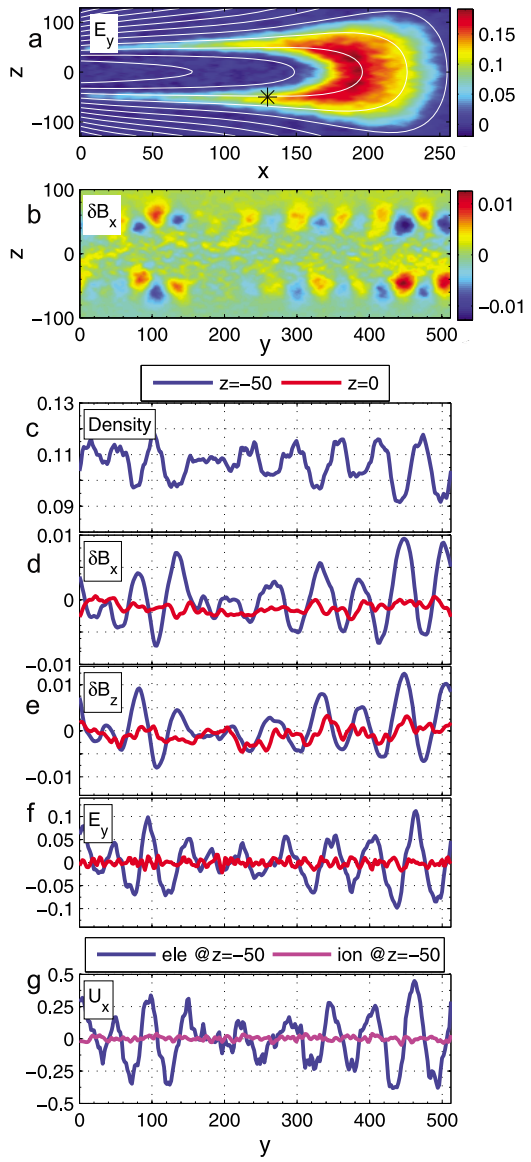

Figure 1. Results from PC2010 run: (a) (X, Z) cut of the Y-component of the electric field at Ωt = 37.5 at y = 464. The white lines are magnetic field lines. (b) (Y, Z) cut of the X-component of the magnetic field oscillations, and Y-cuts of (c) the density, the (d) X- and (e) Z-components of the magnetic field oscillations, (f) the Y component of the electric field, (g) the X-component of the ion (magenta) and electron (blue) velocity at Ωt = 37.5, and x = 130.

interchange instability with mass ratio m_i/m_e = 64 in a tail-like configuration. There was used a box with 256 × 512 × 256 points along the X (tailward), Y (dawnward), and Z (northward) axes. The equatorial field profile (B_Z) was chosen to have a minimum between x = 32 and 96. Correspondingly, the tailward gradient of B_Z was initially set up between x = 96 and 224.

[8] The results shown in Figure 1 are the time averaged quantities over three electron cyclotron periods in order to remove the high-frequency noise in the simulation. They correspond to simulation time Ωt = 37.5 when the instability is still in the linear stage. Figure 1a shows the (x, z)-cut of the electric field Y-component at y = 464. The white lines are magnetic field lines. As mentioned in PC2010, this electric field structure makes clear that the electron flow in the simulation is almost entirely field aligned, demonstrating that the BICI mode is a non-local mode in which significant kinetic ion and electron effects (bounce and drift resonant interactions) are present which are not included in an MHD treatment.

[9] Figure 1b shows an (y, z)-cut of perturbations produced by BICI in the B_X magnetic field component at x = 130 (slightly tailward of B_Z minimum, as marked by the star showing the location of a virtual spacecraft at x = 130, z = −50 in Figure 1a). The perturbations are absent across the neutral sheet, so the mode at this cross-section is mostly confined to the off-equatorial part of the plasma sheet. The peaks above and below the neutral sheet either both increase or both decrease the field, revealing a sausage-like finger structure produced by the kinetic BICI. The perturbations produced by the BICI in B_X and the other fields drift duskward at about one tenth of the ion thermal speed. Due to this drift the Y-profile of perturbations in Figure 1 is nearly equivalent to a temporal plot of parameters that would be observed by a magnetospheric spacecraft.

[10] Figures 4c–4f show Y-cuts of the basic parameters, suggesting duskward propagation of the entire pattern (as observed in simulations); these plots can be directly compared with temporal variations observed in the magnetotail. Note that since at z = 0 the density is constant on the scale of the BICI wavelength and is also much larger than at z = −50, we do not show it in this figure. The oscillations in the magnetic field components δB_X and δB_Z are in phase; those in the electric field E_Y-component are phase shifted by $\pi/2$. The E_Y oscillations are, however, in phase with the X-component of the electron velocity (Figure 1g), which is the largest of the three $\mathbf{U_e}$ components and not accompanied by comparable ion velocity variation. Strong δB_X (compressional) and δN_e, together with phase-shifted δE_Y and δU_{Xe}, reveal distinctive BICI signatures in the cross-section near the B_Z minimum, and the structure of BICI fingers cross-tail-drifting in the westward direction. Note that similar signatures were seen during the non-linear stage of the instability development also (see *Pritchett and Coroniti* [2010] for details).

3. THEMIS Observations of Oscillations Resembling Kinetic BICI Signatures

[11] Figure 2 shows THEMIS probe (P3, P4, and P5) observations on 11 February 2008 between 4:24 and 4:30 UT. The probes were clustered at radial distances between 9.8 and 10.8 R_E downtail. As shown by *Sergeev et al.* [2012], auroral intensification onset at 04:27:08 UT was accompanied by azimuthal striations and was followed by explosive auroral brightening ~10 seconds later, at 04:27:18 UT. At 04:27:30 UT P4 started to observe a fast flow burst and dipolarization. The time delay between observations at P4 and P5 suggests that the associated dipolarization propagated earthward. The probes were located within 1 hour MLT eastward of the auroral breakup arc.

[12] This substorm onset followed 2 min-long strong field and plasma oscillations (period about 20 seconds) observed by P3 and P4 after 04:25:30 UT. Figure 2b shows that the oscillations' amplitudes in the X_{GSM} magnetic field component reached 20 nT at P4. P4 was located between P3, which was in the plasma sheet boundary layer, and P5, which was

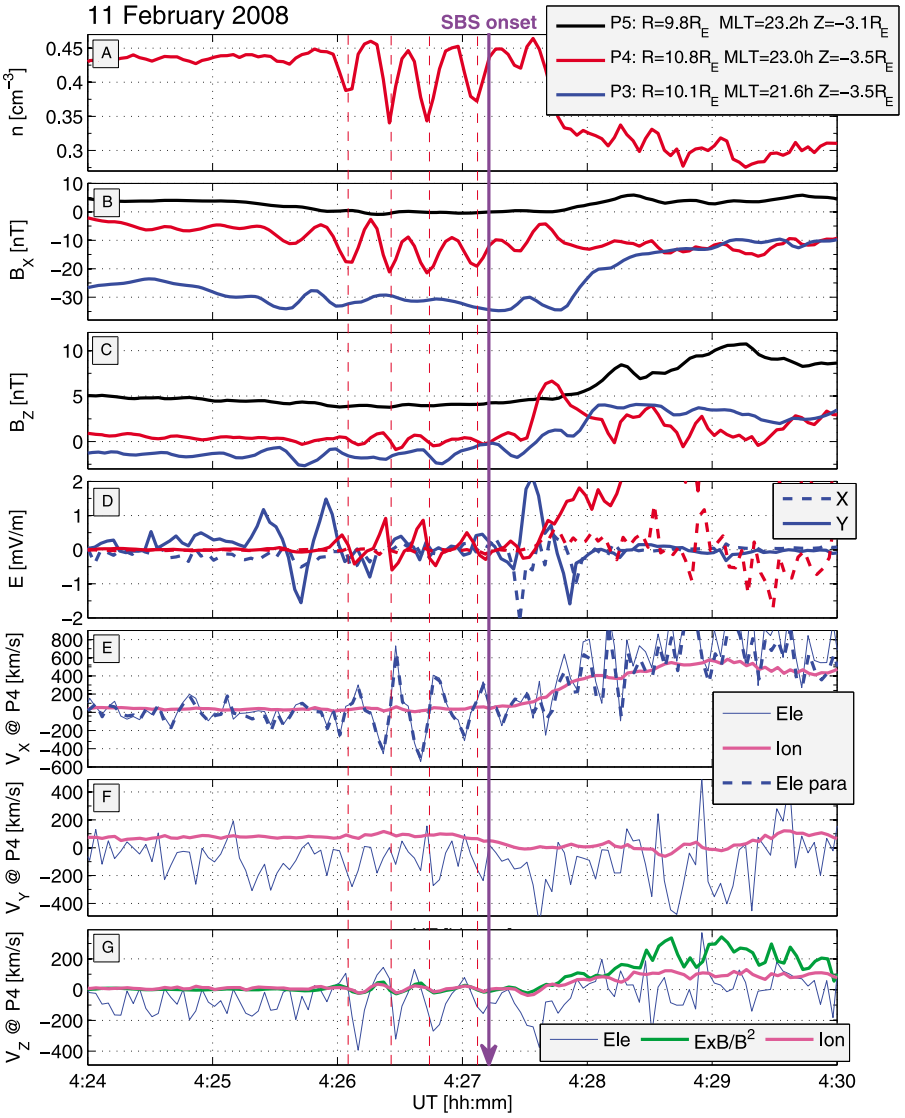

Figure 2. Data from P3, P4, and P5 on 11 February 2008 between 4:24 and 4:30 UT: (a) electron density; (b, c) X_{GSM}- and Z_{GSM}-component of the magnetic field; (d) X_{GSM}- and Y_{GSM}-components of the electric field; (e, f, g) X_{GSM}-, Y_{GSM}-, and Z_{GSM}-components of ion and electron velocity for P4). SBS stands for substorm. See legends for color coding.

in the central plasma sheet. It is interesting that the oscillations at P5 (i.e., in the neutral sheet) did not exceed 2 nT. This suggests that the current sheet oscillations could be sausage-like (i.e., balloons) rather than flap-like structures (i.e., kinks). The oscillations in the perpendicular Y_{GSM}-(not shown) and Z_{GSM} magnetic field components are one order of magnitude smaller than in the field-aligned X_{GSM} magnetic field component. The B_X-oscillations were accompanied by phase-shifted electric field oscillations with the major E_Y-component (Figure 2d), such that $E_Y \sim -\partial B_X/\partial t$ (not shown here).

[13] The intense B_X and E_Y oscillations are typical of the kinetic BICI suggested in PC2010. Another signature of this instability is the oscillating X_{GSM} electron velocity component unaccompanied by corresponding ion velocity oscillations (see Figure 2e). The electron velocity oscillations were in phase with the oscillations in E_Y. It is important to note that the electron velocity oscillations along the X-axis are entirely field aligned (dashed and solid blue curves in Figure 2e repeat each other between 4:26 and 4:27 UT). The oscillations' amplitude in V_Y was much smaller than in V_X. The peak magnitude of V_Z appeared to be comparable to that of V_X. The electron velocity peaked at about 300 to 600 km/s, i.e., at up to 50% of the thermal ion velocity V_{Ti} ($V_{Ti} \approx 1200$ km/s for $T_i \approx 8$ keV). The corresponding field-aligned current densities could reach 40–50 nA/m^2. The strong peaks in electron V_X with amplitudes comparable to V_{Ti} are another essential signature of kinetic BICI (PC2010). A striking feature is that the ion velocity oscillations were one order of magnitude weaker than observed during the flow burst, which can be seen later at 4:28 UT. During the flow burst, ion and electron flows were associated with an intense flux transport and were equally fast. Good correlation between the Z_{GSM}-components of the E × B-drift velocity and the ion velocity during the oscillations (magenta and green curves in Figure 2g) confirms good ion-moment quality.

[14] Figure 3 presents a much longer oscillation event on 28 February 2008 between 7:12 and 7:38 UT (the oscillations started at about 7:00 UT, not shown here). The

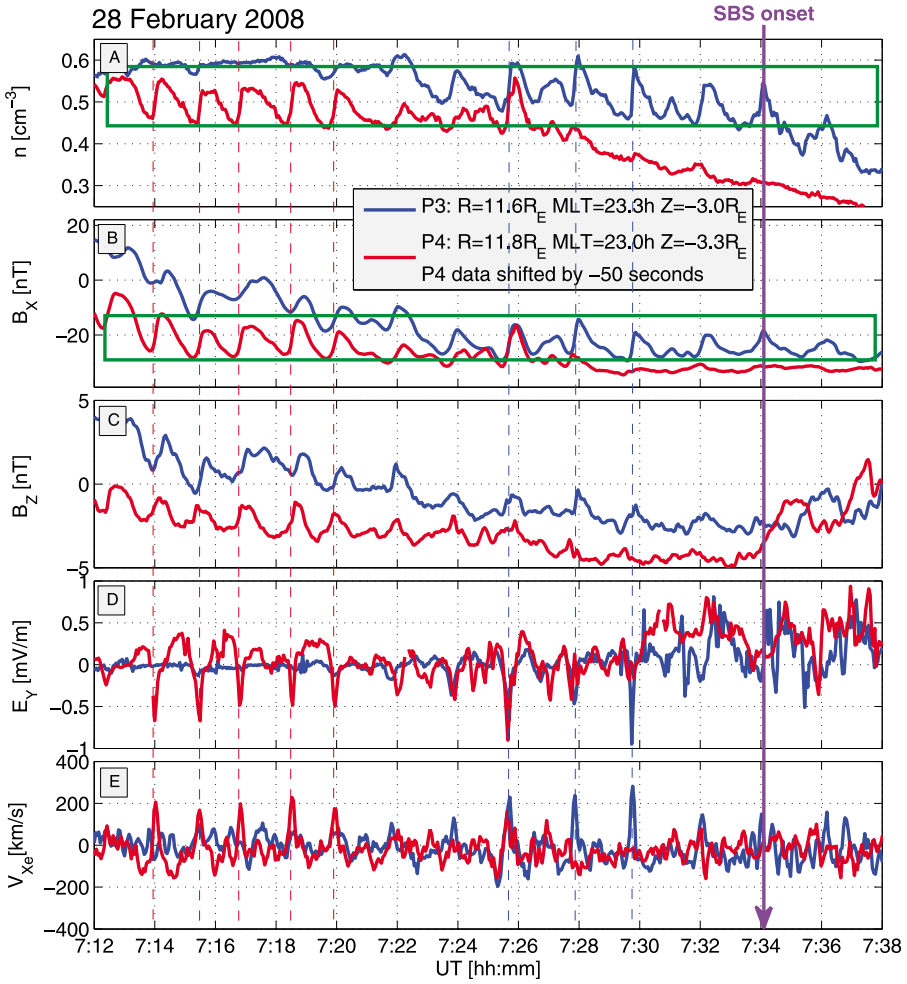

Figure 3. Data from P3 and P4 on 28 February 2008 between 7:12 and 7:38 UT: (a) electron density; (b, c) X_{GSM}- and Z_{GSM}-component of the magnetic field; (d) Y_{GSM}-component of the electric field; (e) X_{GSM}-component of the electron velocity. P4 data are shifted by −50 seconds. See legend for color coding.

observations at P4 (red line) were shifted in time by 50 seconds to highlight the similarity of curves at P3 and P4. Figures 3a and 3b show anti-correlated oscillations of the electron density and the X_{GSM} magnetic field component with a period of ∼100 seconds observed by P3 and P4. Figures 3c–3e show nearly the same BlCl signatures as the observations in Figure 2: smaller-amplitude oscillations in B_Z and large oscillations in E_Y (Figures 3c and 3d). Figure 3e also shows similar oscillations in the X_{GSM}-component of the electron velocity, without comparable ion velocity oscillations (for better visibility we do not show the ion velocity). The electron velocity components have been time averaged over 5 probe spins (15 seconds) to remove high-frequency thermal noise.

[15] In this event, a substorm onset was identified at about 07:34 UT as onset of Pi2 waves and current wedge formation on the ground, together with strong oscillations at GOES-11 (at ∼22.5 h MLT).

[16] There are several notable new features. First, the spiky appearance of the oscillations in the X_{GSM}-component of the electron velocity and the Y_{GSM}-component of the electric field is correlated with the asymmetric (sawtooth) shape of the magnetic field oscillations (steeper rises and sloping drops in B_X). This correlation also highlights the synchronization between the negative E_Y peaks and the positive V_X peaks.

[17] Second, the long duration of the oscillations and different locations of P3 and P4 with respect to the neutral sheet allowed us to see that spiky E_Y, V_X and density oscillations were substantially weaker both near the neutral sheet (large density ∼0.6 cm^{-3} and small $|B_X|$ amplitude) and in the lobes (density was below 0.4 cm^{-3} and $|B_X|$ exceeded 30 nT). We indicated the region of largest oscillation amplitudes between the plasma sheet center and its outer edge with a green rectangle in Figures 3a and 3b.

[18] Third, in this event P3 and P4 were separated by 5950 km mostly along the Y_{GSM}-axis. Long-lasting oscillations allowed us to compute the cross-correlation of the signals from P3 and P4, which gave a distinct peak at 50 seconds and indicated duskward propagation at a velocity of about 120 km/s. The characteristic cross-tail scale for the half-period of T = 50 seconds is then 6000 km.

[19] Using the AM-03 model [*Kubyshkina et al.*, 2011] it was shown that the oscillations on 11 February 2008

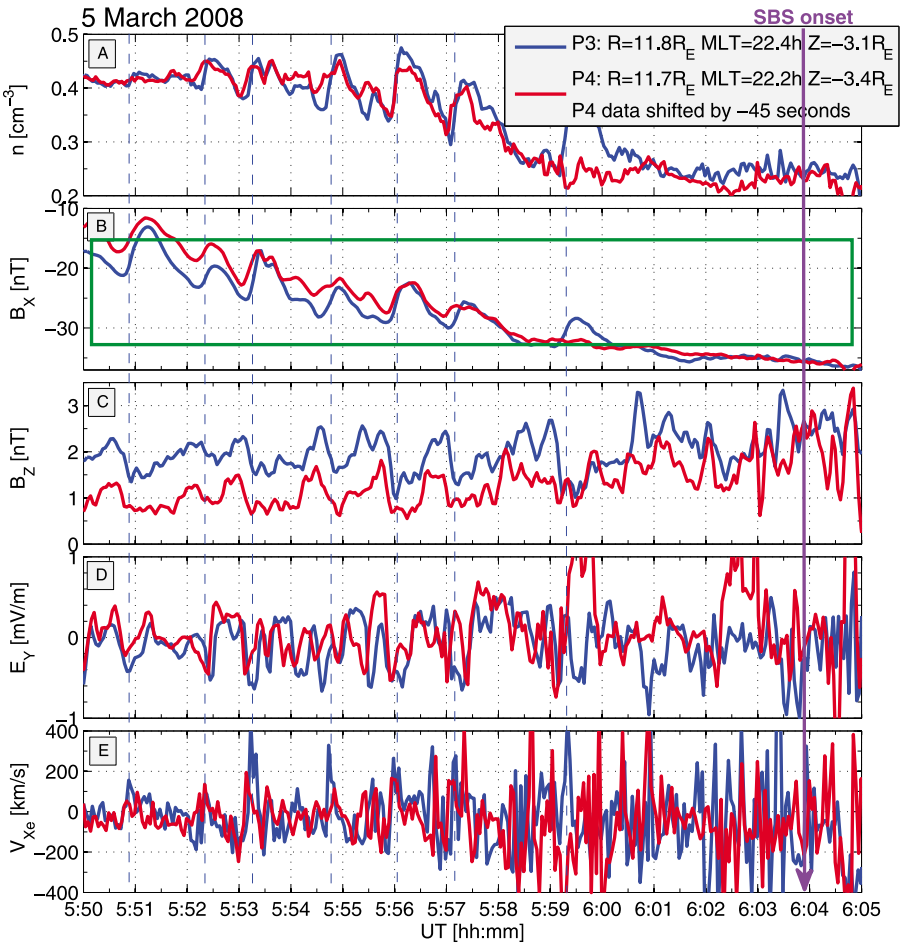

Figure 4. Same as in Figure 3 for THEMIS observations on 5 March 2008 between 5:50 and 6:05 UT. P4 data are shifted by −45 seconds.

and on 28 February 2008 were observed in the stretched parts of the magnetotail, which were nearly horizontally oriented in the GSM coordinates [*Sergeev et al.*, 2012; *E. V. Panov et al.*, Kinetic ballooning/interchange instability in a bent plasma sheet, submitted to Journal of Geophysical Research, 2012].

[20] Figure 4 shows THEMIS observations on 5 March 2008. Similar oscillations were found after 5:50 UT and before the auroral breakup at 06:04 UT. This event was reported by *Uritsky et al.* [2009], who focused on conjugate ground all-sky camera observations of azimuthally-drifting auroral waves. They noticed a time shift between the oscillations at P3 and P4 and interpreted the oscillations as flapping (kink) waves propagating duskward at a velocity between 90 and 100 km/s. The character of these oscillations is similar to those in the events previously mentioned. The observations at P4 (red line) were shifted in time by 45 seconds to highlight the similarity of curves at P3 and P4. This assured us that the oscillations were a relatively long-lived spatial pattern drifting duskward. A 45 seconds time delay over cross-tail separation of 5500 km suggests a 120 km/s propagation speed (similar to that from the observations on 28 February 2008). The characteristic cross-tail scale for the T = 38 seconds half-period would then be 4500 km. The 5 March 2008 observations are also morphologically similar to those on 28 February 2008: in both events, THEMIS probes observed sawtooth-shaped B_X oscillations and spiky E_Y and V_X patterns as well as confinement of the oscillations to a region between the neutral sheet and the boundary layer.

4. Discussion and Conclusions

[21] In this paper we show THEMIS observations of field and plasma oscillations at 11 R_E prior to breakup. Detailed comparison of these observations with the PIC simulation run from PC2010 suggests that the oscillations grew during development of a kinetic ballooning/interchange instability. In particular, we find agreement regarding the strong dominance of the electron V_X oscillations over the ion velocity oscillations; the general sausage character of the mode perturbations; and the frequency, wavelength, and duskward velocity drift of the oscillations. The oscillations drifted duskward at about 120 km/s, and their wavelengths were about nine to twelve thousand km, comparable to a gyroradius of 10 keV ion in $B \sim 2$ nT.

[22] Although we are unaware of any theoretical study which could suggest that similar signatures may appear during the development of another than the BICI instability, it is important to keep this possibility open.

[23] There are also several disagreements between the simulations and THEMIS observations. Whereas in

THEMIS observations δB_X was observed to be very strong between the neutral sheet and the lobes (up to 50% of the lobe field), it did not exceed 5% of the lobe field in the PC2010 run. The amplitude of δB_X may, however, depend on other parameters, such as the plasma beta and ion-to-electron mass ratio; this should be further investigated. Note that in the PC2010 run, a large value for the initial B_Z field was chosen because of numerical constraints.

[24] BICI growth is expected in the region of the tailward gradient of B_Z (PC2010). Such reversed $\partial B_Z/\partial X$ can appear, e.g., tailward of a magnetic field minimum B at the outer edge of dipole-like magnetic field region [*Saito et al.*, 2010]. Identification of such plasma sheet configurations with sparse spacecraft coverage is a challenge. Nevertheless, the Z_{GSM}-component of the magnetic field was rather small, less than 1–2 nT at about 11 R_E downtail. This is consistent with a larger magnetic field farther downtail (with a local minimum B at around 11 R_E) required to explain the large auroral oval width, >5° of the magnetic latitude. Although not a rigorous proof, this argument suggests that the assumption of a local magnetic field minimum is reasonable and would would link observations with PC2010 simulation results.

[25] An important conclusion from our results is that the observed entirely field-aligned electron V_X oscillations and decoupling of the electron and ion flows clearly demonstrate that the BICI mode contains features that cannot be explained by a fluid treatment and suggest that electron kinetics should not be neglected in future theoretical studies of ballooning/interchange instability in the Earth's plasma sheet.

[26] Also, *Pritchett and Coroniti* [2011] have shown that under some circumstances the kinetic ballooning/interchange instability can provoke reconnection onset. As was demonstrated by *Uritsky et al.* [2009], *Sergeev et al.* [2012] and *Panov et al.* (submitted manuscript, 2012) in all the THEMIS events considered above, oscillations ended with a substorm onset. Although reconnection was observed in all three events, in the 28 February 2008 event the oscillations persisted over tens of ion gyroperiods without a substorm onset, suggesting that the BICI does not always immediately lead to magnetotail reconnection. Therefore more realistic simulation runs of BICI should be compared with additional *in situ* observations of BICI to study the operational region, the growth conditions, different phases and non-linear effects of instability development, and how instability relates to substorm onset.

[27] **Acknowledgments.** We acknowledge NASA contract NAS5-02099 for use of data from the THEMIS Mission. Specifically: U. Auster for use of FGM data provided under the lead of the Technical University of Braunschweig and with financial support through the German Ministry for Economy and Technology and the German Center for Aviation and Space (DLR) under contract 50 OC 0302; C. W. Carlson for use of ESA data; J. W. Bonnell and F. S. Mozer for use of EFI data. The work was partly supported by the Austrian Science Fund (FWF) I429-N16, by the Seventh Framework European Commission Programme (FP7, project 269198 - 'Geoplasmas'), and by NASA grant NNX10AK98G. The PIC simulations were made possible by the NASA Advanced Supercomputing (NAS) Division at the Ames Research Center. E.V.P. thanks A. A. Petrukovich and A.V. Artemyev for fruitful discussion. The authors acknowledge J. Hohl for helping with editing and thank the reviewers for initiating interesting discussions and useful comments which have helped to improve the paper.

[28] The Editor thanks an anonymous reviewer for assisting with the evaluation of this paper.

References

Angelopoulos, V. (2008), The THEMIS Mission, *Space Sci. Rev.*, *141*, 5–34, doi:10.1007/s11214-008-9336-1.

Auster, H. U., et al. (2008), The THEMIS Fluxgate Magnetometer, *Space Sci. Rev.*, *141*, 235–264, doi:10.1007/s11214-008-9365-9.

Baumjohann, W., et al. (2007), Dynamics of thin current sheets: Cluster observations, *Ann. Geophys.*, *25*, 1365–1389, doi:10.5194/angeo-25-1365-2007.

Bonnell, J. W., F. S. Mozer, G. T. Delory, A. J. Hull, R. E. Ergun, C. M. Cully, V. Angelopoulos, and P. R. Harvey (2008), The electric field instrument (EFI) for THEMIS, *Space Sci. Rev.*, *141*, 303–341.

Cheng, C. Z., and A. T. Y. Lui (1998), Kinetic ballooning instability for substorm onset and current disruption observed by AMPTE/CCE, *Geophys. Res. Lett.*, *25*, 4091–4094, doi:10.1029/1998GL900093.

Elphinstone, R. D., et al. (1995), Observations in the vicinity of substorm onset: Implications for the substorm process, *J. Geophys. Res.*, *100*, 7937–7969, doi:10.1029/94JA02938.

Kubyshkina, M., V. Sergeev, N. Tsyganenko, V. Angelopoulos, A. Runov, E. Donovan, H. Singer, U. Auster, and W. Baumjohann (2011), Time-dependent magnetospheric configuration and breakup mapping during a substorm, *J. Geophys. Res.*, *116*, A00I27, doi:10.1029/2010JA015882.

Liang, J., E. F. Donovan, W. W. Liu, B. Jackel, M. Syrjäsuo, S. B. Mende, H. U. Frey, V. Angelopoulos, and M. Connors (2008), Intensification of preexisting auroral arc at substorm expansion phase onset: Wave-like disruption during the first tens of seconds, *Geophys. Res. Lett.*, *35*, L17S19, doi:10.1029/2008GL033666.

McFadden, J. P., C. W. Carlson, D. Larson, V. Angelopoulos, M. Ludlam, R. Abiad, B. Elliot, P. Turin, and M. Marckwordt (2008), The THEMIS ESA plasma instrument and in-flight calibration, *Space Sci. Rev.*, *141*, 277–302.

Miyashita, Y., et al. (2009), A state-of-the-art picture of substorm-associated evolution of the near-Earth magnetotail obtained from superposed epoch analysis, *J. Geophys. Res.*, *114*, A01211, doi:10.1029/2008JA013225.

Ohtani, S.-I. (2004), Flow bursts in the plasma sheet and auroral substorm onset: Observational constraints on connection between midtail and near-Earth substorm processes, *Space Sci. Rev.*, *113*, 77–96, doi:10.1023/B:SPAC.0000042940.59358.2f.

Pritchett, P. L., and F. V. Coroniti (2010), A kinetic ballooning/interchange instability in the magnetotail, *J. Geophys. Res.*, *115*, A06301, doi:10.1029/2009JA014752.

Pritchett, P. L., and F. V. Coroniti (2011), Plasma sheet disruption by interchange-generated flow intrusions, *Geophys. Res. Lett.*, *38*, L10102, doi:10.1029/2011GL047527.

Roux, A., S. Perraut, P. Robert, A. Morane, A. Pedersen, A. Korth, G. Kremser, B. Aparicio, D. Rodgers, and R. Pellinen (1991), Plasma sheet instability related to the westward traveling surge, *J. Geophys. Res.*, *96*, 17,697–17,714, doi:10.1029/91JA01106.

Saito, M. H., Y. Miyashita, M. Fujimoto, I. Shinohara, Y. Saito, and T. Mukai (2008), Modes and characteristics of low-frequency MHD waves in the near-Earth magnetotail prior to dipolarization: Fitting method, *J. Geophys. Res.*, *113*, A06201, doi:10.1029/2007JA012778.

Saito, M. H., L.-N. Hau, C.-C. Hung, Y.-T. Lai, and Y.-C. Chou (2010), Spatial profile of magnetic field in the near-Earth plasma sheet prior to dipolarization by THEMIS: Feature of minimum B, *Geophys. Res. Lett.*, *37*, L08106, doi:10.1029/2010GL042813.

Sergeev, V., Y. Nishimura, M. Kubyshkina, V. Angelopoulos, R. Nakamura, and H. Singer (2012), Magnetospheric location of the equatorward prebreakup arc, *J. Geophys. Res.*, *117*, A01212, doi:10.1029/2011JA017154.

Uritsky, V. M., J. Liang, E. Donovan, E. Spanswick, D. Knudsen, W. Liu, J. Bonnell, and K. H. Glassmeier (2009), Longitudinally propagating arc wave in the pre-onset optical aurora, *Geophys. Res. Lett.*, *36*, L21103, doi:10.1029/2009GL040777.